Dual-wavelength InP quantum dot lasers

S. Shutts, P. M. Smowton, and A. B. Krysa

Dual-wavelength InP quantum dot lasers

S. Shutts,[1] P. M. Smowton,[1] and A. B. Krysa[2]

[1]School of Physics and Astronomy, Cardiff University, Cardiff CF24 3AA, United Kingdom
[2]EPSRC National Centre for III-V Technologies, Department of Electronic and Electrical Engineering, University of Sheffield, Mappin Street, Sheffield S1 3JD, United Kingdom

We have demonstrated a two-section dual-wavelength diode laser incorporating distributed Bragg reflectors, with a peak-wavelength separation of 62.5 nm at 300 K. Each lasing wavelength has a different temperature dependence, providing a difference-tuning of 0.11 nm/K. We discuss the mechanisms governing the light output of the two competing modes and explain how the short wavelength can be relatively insensitive to output changes at the longer wavelength. Starting from an initial condition when the output at both wavelengths are equal, a 500% increase in the long wavelength output causes the short wavelength output to fall by only 6%. © 2014 Author(s). All article content, except where otherwise noted, is licensed under a Creative Commons Attribution 3.0 Unported License. [http://dx.doi.org/10.1063/1.4883857]

Dual-wavelength (dual-λ) lasers are required for a number of applications that include distance and position interferometric measurements, as sources in read/write devices for optical storage and bio-photonic applications. Techniques such as laser speckle contrast imaging (LSI) and 2D photoacoustic imaging use pulsed dual-λ lasers to study multiple vascular physiological parameters such as concentration of haemoglobin, blood flow and oxygen saturation.[1] Here, we focus on using a structure that exploits quantum dot (QD) properties to achieve lasers that emit at two well-defined wavelengths at the same time and on the same optical axis.

Simultaneous dual-state lasing in the same spatial location is usually difficult to achieve or to control in a semiconductor material because stimulated recombination processes at a particular energy compete for carriers undergoing similar processes at other energies. Simple semiconductor lasers will emit two or more wavelengths, but generally emit with one dominating wavelength. Several approaches have been suggested to produce more reliable dual-λ operation. Many of these rely on lasing in a different spatial position to avoid or mitigate the direct competition for excited carriers [e.g., Refs. 2 and 3]. However, lasing at slightly different spatial positions can produce complications in many of the applications that require two wavelengths. An effort to combine two wavelengths into a single emitting arm has been achieved using Y-branch lasers.[4] But the disadvantage of these devices is that they have a larger footprint than normal laser diodes and require careful design of the out-coupler to prevent back-reflections into opposing arms of the Y-branch, which otherwise creates instability in the output. Ridge waveguides incorporating two grating regions with different Bragg-wavelengths and a common gain section have been successfully used to generate emission at two closely spaced wavelengths with narrow line widths.[5] However, the various sections of such devices are not electrically isolated and this can lead to superfluous pumping of adjacent sections. In addition, shallow etched gratings tuned to one wavelength can cause scattering loss at the other lasing wavelength and lead to vertical guiding, which tends to spatially separate the two propagating modes. We aimed to circumvent these

issues by fabricating a device comprising two electrically independent sections with a deep-etched Distributed Bragg Reflector (DBR) grating acting as a partition between the sections. The use of a deep-etched grating brings several key advantages. First, the refractive index in the vertical direction (normal to the growth plane) is symmetric on the scale of the optical mode, meaning the allowed modes are not offset towards the substrate, as observed with shallow-etched gratings. Second, a high reflectivity at one wavelength can be achieved using few periods, whilst providing high transmittance at other wavelengths with minimal scattering. The role of the DBR in achieving dual-λ emission and how its design affects device performance will be discussed.

For truly independent lasing at the same spatial location, the modes must not interact with the same set or pool of excited electrons and so must be separated in energy by more than the homogenous linewidth.[6] In addition, carriers must not be able to move between the two carrier pools, or the states in which they exist, on a shorter timescale than the recombination process that removes carriers from those excited states. The latter requirement, equivalent to a lack of a thermal equilibrium between the energy states, is difficult to achieve in most semiconductors, but can be met using QDs.[7] This has led to the demonstration of dual-λ lasing in QD material.[8,9]

There are further additional criteria that are necessary for optimum dual-λ performance. Clearly, population inversion must be achieved over an energy range large enough to encompass the two lasing photon energies and when using a single active material this comes with the penalty of an increased current density, which can be significant for widely spaced wavelengths. In some of the envisioned applications, it would be useful to independently control the wavelengths, so that the device may be operated with both wavelengths emitting simultaneously or individually. It is also useful to have some tuning capability to either actively stabilise or to set the difference-wavelength.

In this work, we describe a semiconductor lasing device to meet at least some of the aforementioned requirements, which was designed to exploit the properties of InP quantum

104, 241106-1

dots grown on GaAs substrates that potentially cover the 650–780 nm wavelength range.[10]

The InP QD laser structure was grown by low pressure metal-organic vapour phase epitaxy (MOVPE) on an n-GaAs (100) substrate oriented 10° toward ⟨111⟩. The sample was grown at 730 °C using trimethyl precursors for the group III elements and arsine AsH$_3$ and phosphine PH$_3$ as precursors of the group V elements. Self-assembled dots were formed from the equivalent of 3 monolayers of InP material deposited on (Al$_{0.3}$Ga$_{0.7}$)$_{0.51}$In$_{0.49}$P and covered with 8 nm Ga$_{0.54}$In$_{0.46}$P quantum wells (QWs). Using a composition of Ga$_x$In$_{1-x}$P that is tensile strained compared to the underlying substrate reduces the current density required to achieve lasing on the quantum dot states as described in Ref. 11. The structure contained 5 layers of dots in wells (D-WELL) where each D-WELL layer was separated by 16 nm wide (Al$_{0.3}$Ga$_{0.7}$)$_{0.51}$In$_{0.49}$P barrier layers. 1000 nm wide Al$_{0.51}$In$_{0.49}$P cladding layers, doped with Si and Zn for n and p-type, respectively, formed the rest of the waveguide structure.

Modal gain spectra measured using a stripe-length method[12] are plotted in Figure 1 for increasing current density. Such broad gain spectra are typically observed for quantum dot material. In addition to the increase in gain magnitude with increasing carrier injection, there is a blue shift of the gain-peak wavelength due to state-filling of the inhomogenously broadened dot states. Therefore, it is the value of gain required, or equivalently the cavity loss (per unit length), which determines the absolute peak wavelength.

To achieve dual-λ lasing in the same spatial location, we employ a monolithic device, represented in schematic form in Figure 2, consisting of two sections that can be independently electrically driven and separated by a DBR. This DBR is designed to be reflective at the shorter of the two lasing wavelengths and transparent at the longer wavelength. A second DBR, which is reflective at the longer lasing wavelength, is placed at the rear of the device. The first laser cavity (section one) is formed by the front cleaved facet and the DBR located between the two sections, and the second cavity (section one plus section two) is formed from the front facet and the back DBR. The inhomogeneous broadening
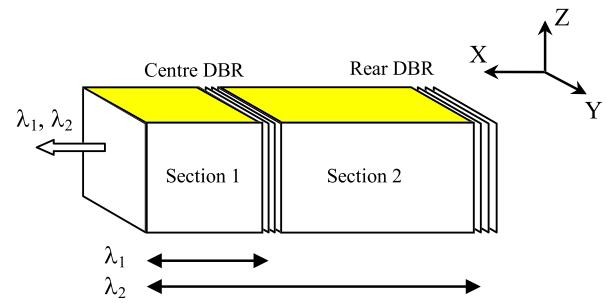

FIG. 2. Schematic diagram of device structure.

introduced by the dot material allows simultaneous operation at the two wavelengths. The short cavity formed by section one has a relatively high optical loss per unit length and therefore emits at a shorter wavelength (utilising higher energy states). The second cavity has a relatively low optical loss and lasers on a longer wavelength utilising lower energy states. The electrical isolation of the two sections is achieved by etching the gaps in the grating portions down to the substrate, which also ensures that there is minimal vertical (Z) variation in refractive index through the optical waveguide. In lasers incorporating surface gratings, the variation in refractive index has the effect of pushing the optical mode down towards the substrate and the degree to which this occurs is wavelength dependent, causing a small spatial offset between the two lasing wavelengths. Measurements of the lateral and transverse near-fields performed on these devices revealed that the optical modes associated with both wavelengths co-exist in the same spatial region. The characteristic FWHM of the transverse (z-direction) far-field distributions of both wavelengths were found to be very similar at 45° and 48 ± 1.5° for the long and short, respectively. Time-resolved images of emission spectra (obtained using a streak camera) indicate that the two lasing modes emit simultaneously when applying the appropriate injection ratio.

The Bragg gratings used here were based on third order quarter-wave stacks and the peak of the centre grating stop-band is positioned such that the reflectivity, or feedback, is higher at shorter wavelengths. In doing so, the loss of the cavity and the emission wavelength is influenced by both its length and the nature of the reflectivity spectrum attributed to the centre grating.

To achieve the largest wavelength separation, a grating structure was designed where the reflectively is only above that of a cleaved facet at the short wavelength limit of the material, accessed by high injection. An example of a centre grating reflectivity spectra used to achieve a large wavelength separation is shown in the inset to Figure 3. The high-loss laser operates on the long wavelength edge of the stop-band at approximately 658 nm, and the low-loss laser operates through the minimum in the reflectivity at approximately 720 nm.

The overall mirror loss ($\alpha_m(\lambda)$) of the section one is dependent on its length (L_c) and the reflectivity of both the cleaved facet (R_f) and the DBR grating ($R_G(\lambda)$)
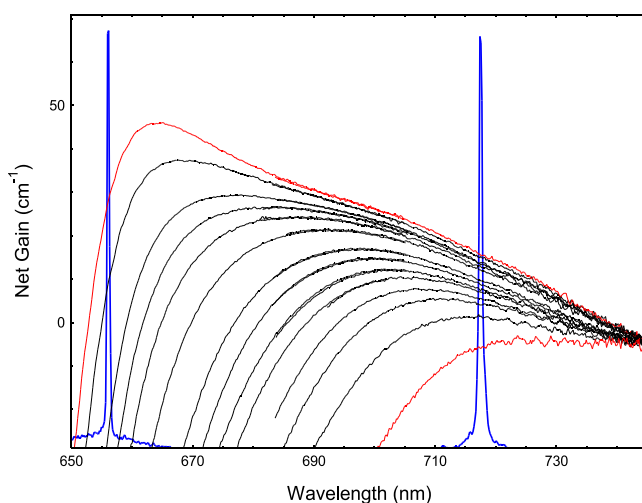

FIG. 1. Measured net modal gain spectra (G-α_i), for increasing current density at 300 K with lasing spectrum of dual-λ laser superimposed. The difference-λ is 62.5 nm.
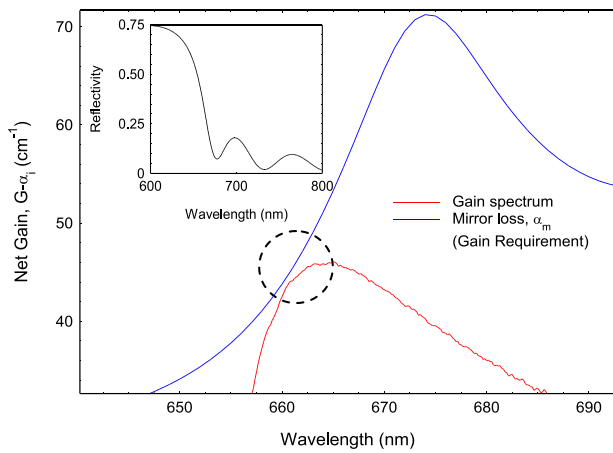
$$\alpha_m(\lambda) = \frac{1}{2L_C}\ln\left(\frac{1}{R_f R_G(\lambda)}\right). \qquad (1)$$

FIG. 3. Peak of the net modal gain spectra (G-α_i) plotted with mirror loss spectra (α_m) obtained from Eq. (1) using the reflectivity spectrum of inset. When the level of pumping is sufficient, the gain meets the loss spectra (inside dashed circle) and laser action occurs.

This equates to the net-gain requirement, which must be achieved in order for laser action to take place. This spectrally dependent mirror loss is shown in the main part of Figure 3, together with a gain spectrum obtained at high injection. When the level of pumping is sufficient, the gain curve meets the loss spectrum. The point at which this occurs corresponds to the wavelength at which a laser would emit under these conditions and it does not necessarily coincide with the material gain-peak wavelength. The gain requirement (or mirror loss) at wavelengths above this dramatically increases and hence lasing at longer wavelengths is not possible. This method of modifying the loss spectrum of section one using the centre grating allows for a large separation of lasing wavelengths.

In Figure 1, the spectrum resulting from driving sections one and two at 120 mA (3.3 kA cm^{-2}) and 35 mA (230 A cm^{-2}), respectively, is superimposed over the gain spectra measured at 300 K. At this temperature, the lasing wavelength separation achieved is 62.5 nm. As described in Eq. (1), the mirror loss is inversely proportional to the cavity length. It will be appreciated that by varying the optical-mirror loss of section one, by either altering its length or the reflectivity stop-band of the centre DBR, the difference-wavelengths can be altered. The ability to source a wide range of wavelengths is made possible by the large gain bandwidth, resulting from the large inhomogeneous distribution in dot size.

In QD material, the temperature dependence of emission wavelengths varies with the optical-loss of the laser as described in Ref. 13. Since the two wavelengths are selected by using different optical-losses, they have a different temperature dependence, and this means that the separation of the lasing wavelengths can be fine-tuned using the operating temperature. This is modified somewhat compared to the results obtained in Ref. 13, because the reflectivity of the DBR is also temperature dependant. The temperature tuning of the difference-wavelength is approximately linear with temperature and varies at $\approx$0.11 nm/K for a laser with a 300 K wavelength separation of 62.5 nm.

It is apparent that the stability, or range of pumping conditions over which dual-mode operation can be achieved is dependent on the difference in the gain requirement of the two modes, the way carriers distribute amongst the dot states involved, and how effectively the centre grating operates as a selective filter.

To investigate the intensity stability at the two wavelengths, the light level from each mode was initially set to be equal (by adjusting the current to sections one and two), and then the fractional change in light at each mode was monitored as the current in one of the two sections was varied, while the other was held constant. Figure 4 shows that the light level at the short wavelength remains relatively fixed for changes in current applied to section two. Conversely, varying the current applied to section one causes the light output at both wavelengths to change. The latter is due to two effects; first, increasing the current in section one increases the number of carriers available to recombine at each wavelength, and second, a proportion of the light generated from the high energy states of section one is transmitted through the centre DBR optically pumping section two. The gain requirement of the mode, which emits at the long wavelength, is relatively low, and so the level of injection required to reach threshold is much less than that of the short wavelength. Moreover, above threshold, the variation of light output to changes in carrier injection are more sensitive in a laser operating at a low carrier density, and this effect can be further explained by considering the light-current characteristics. With reference to the inset in Figure 4, which illustrates the difference in slope efficiencies of the two modes, a low-loss (long wavelength) laser operating at a low level of injection will have an external differential efficiency, which is greater than a high-loss (short wavelength) laser. Above threshold, the fractional change in light with carrier density will be less for a high-loss (short wavelength) cavity. In the device shown, the slope efficiency for the long wavelength emission is 3 times greater than that of the short wavelength. Furthermore, only a fraction of the total carriers recombining at the long wavelength are acquired from section one, and with the low level
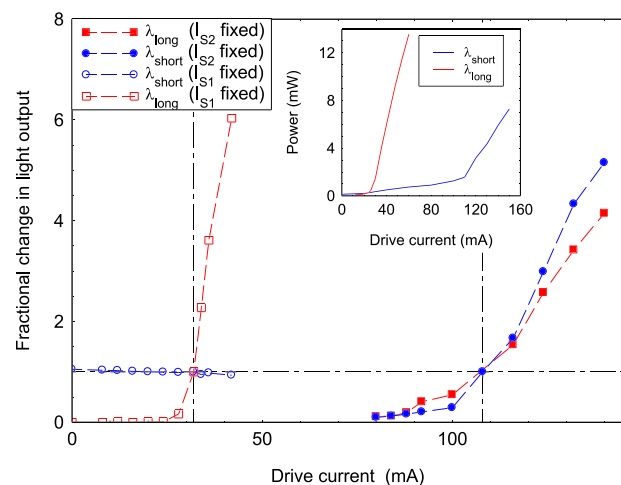

FIG. 4. Fractional change in light intensity at each wavelength (λ_1, λ_2) when fixing the current (I) in one section while varying the current applied to other. Point at which the dashed lines cross corresponds to initial conditions where the light intensity in each mode was equal. Inset shows light-current characteristic of the two lasing modes, with horizontal axis corresponding to total current of section one (blue line) and section one plus two (red line).

of inversion required for lasing at the long wavelength, the carrier competition in that section is minimal.

We have described a simple structure to generate dual-λ lasing in the same spatial and temporal position, with a wavelength separation of up to 62.5 nm demonstrated. We have shown how the two wavelengths are set using the optical loss of each cavity and how the difference in lasing wavelength can be fine tuned using the operating temperature. The stability of each dominating mode, to changes in drive current, was assessed by measuring the fractional variation in light output. Results indicate that the short wavelength emission is relatively insensitive to variations in light at the long wavelength. Conversely, the light output of the long wavelength is affected by changes in output at the short wavelength, but this can be compensated for by modulating the current supplied to section two of the device.

[1]J. Qin, R. Reif, Z. Zhi, S. Dziennis, and R. Wang, "Hemodynamic and morphological vasculature response to a burn monitored using a combined dual-wavelength laser speckle and optical microangiography imaging system," Biomed. Opt. Express **3**(3), 455–466 (2012).

[2]F. Pozzi, R. M. De La Rue, and M. Sorel, "Dual wavelength InAlGaAs-InP laterally coupled distributed feedback laser," IEEE Photonics Technol. Lett. **18**(24), 2563–2565 (2006).

[3]S. Ito, M. Suehiro, T. Hirata, and T. Hidaki, "Two longitudinal-mode laser diodes," IEEE Photonics Technol. Lett. **7**, 959–961 (1995).

[4]R. K. Price, V. B. Verma, K. E. Tobin, V. C. Elarde, and J. J. Coleman, "Y-branch surface etched distributed Bragg reflector lasers at 850 nm for optical heterodyning," IEEE Photonics Technol. Lett. **19**(20), 1610–1612 (2007).

[5]S. D. Roh, R. B. Swint, A. M. Jones, T. S. Yeoh, A. E. Huber, J. S. Hughs, and J. J. Coleman, "Dual-wavelength asymmetric cladding InGaAs-GaAs ridge waveguide distributed Bragg reflector lasers," IEEE Photonics Technol. Lett. **11**(1), 15–17 (1999).

[6]M. Sugawara, K. Mukai, Y. Nakata, K. Otsubo, and H. Ishikawa, "Performance and physics of quantum dot lasers with self assembled columnar shaped and 1.3 μm emitting InGaAs quantum dots," IEEE J. Sel. Top. Quantum Electron. **6**(3), 462–474 (2000).

[7]I. O'Driscoll, P. Blood, and P. M. Smowton, "Random population of quantum dots in InAs-GaAs laser structures," IEEE J. Quantum Electron. **46**, 525–532 (2010).

[8]N. A. Naderi, F. Grillot, K. Yang, J. B. Wright, A. Gin, and L. F. Lester, "Two color multi-section quantum dot distributed feedback laser," Opt. Express **18**(26), 27028–27035 (2010).

[9]N. S. Daghestani, M. A. Cataluna, G. Ross, and M. J. Rose, "Compact dual-wavelength InAs/GaAs quantum dot external-cavity laser stabilized by a single volume Bragg grating," IEEE Photonics Technol. Lett. **23**(3), 176–178 (2011).

[10]P. M. Smowton, J. Lutti, G. M. Lewis, A. B. Krysa, J. S. Roberts, and P. A. Houston, "InP–GaInP quantum-dot lasers emitting between 690–750 nm," IEEE J. Sel. Top. Quantum Electron. **11**, 1035–1040 (2005).

[11]S. N. Elliott, P. M. Smowton, A. B. Krysa, and R. Beanland, "The effect of strained confinement layers in InP self-assembled quantum dot material," Semicond. Sci. Technol. **27**, 094008 (2012).

[12]P. Blood, G. M. Lewis, P. M. Smowton, H. D. Summers, J. D. Thomson, and J. Lutti, "Characterisation of semiconductor laser gain media by the segmented contact method," IEEE J. Sel. Top. Quantum Electron. **9**(5), 1275–1282 (2003).

[13]S. Shutts, P. M. Smowton, and A. B. Krysa, "InP quantum dot lasers with temperature insensitive operating wavelength," Appl. Phys. Lett. **103**, 061106 (2013).